Epithelial sodium channel is a key mediator of growth hormone-induced sodium retention in acromegaly.

Peter Kamenicky, Say Viengchareun, Anne Blanchard, Geri Meduri, Philippe Zizzari, Martine Imbert-Teboul, Alain Doucet, Philippe Chanson, Marc Lombès

Epithelial Sodium Channel is a Key Mediator of Growth Hormone–Induced Sodium Retention in Acromegaly

Peter Kamenicky[1,2], Say Viengchareun[1,2], Anne Blanchard[3], Geri Meduri[1,2,4], Philippe Zizzari[5], Martine Imbert-Teboul[6], Alain Doucet[6], Philippe Chanson[1,2,7], Marc Lombès[1,2,7] *

1- Inserm, U693, Le Kremlin Bicêtre, F-94276, France;
2- Univ Paris-Sud 11, Faculté de Médecine Paris-Sud, UMR-S693, Le Kremlin Bicêtre, F-94276, France;
3- Assistance Publique-Hôpitaux de Paris, Hôpital Européen Georges Pompidou, Centre d'Investigation Clinique, F-75908, Paris, France;
4- *Assistance Publique-Hôpitaux de Paris, Hôpital de Bicêtre, Service de Pharmacogénétique, Biochimie Moléculaire et Hormonologie, Le Kremlin Bicêtre, F-94275, France;*
5- *Inserm, U549, Centre Broca, Paris, F-75014, France;*
6- *CNRS/UPMC, UMR7134, Institut des Cordeliers, Paris, F-75006, France;*
7- *Assistance Publique-Hôpitaux de Paris, Hôpital de Bicêtre, Service d'Endocrinologie et Maladies de la Reproduction, Le Kremlin Bicêtre, F-94275, France.*

Short title: Antinatriuretic action of growth hormone

Key Words: growth hormone, kidney, sodium homeostasis, acromegaly

Disclosure statement: Part of this study was supported by a research grant from Pfizer laboratory (2008-2009, to PC and ML). PC is a consultant of and received lecture fees from Novartis, Pfizer and Ipsen Laboratories.

* Corresponding author:

Marc LOMBES, MD, PhD
Inserm U693, Faculté de Médecine Paris-Sud
63, rue Gabriel Péri, 94276 Le Kremlin Bicêtre Cedex France

Tel: 33 1 49 59 67 09,
Fax: 33 1 49 59 67 32
Email: marc.lombes@u-psud.fr

Abstract

Acromegalic patients present with volume expansion and arterial hypertension but the renal sites and molecular mechanisms of direct antinatriuretic action of growth hormone (GH) remain unclear. Here, we show that acromegalic GC rats, which are chronically exposed to very high levels of GH, exhibited a decrease of furosemide-induced natriuresis and an increase of amiloride-stimulated natriuresis compared to controls. Enhanced Na^+,K^+-ATPase activity and altered proteolytic maturation of epithelial sodium channel (ENaC) subunits in the cortical collecting ducts (CCD) of GC rats provided additional evidence for an increased sodium reabsorption in the late distal nephron under chronic GH excess. *In vitro* experiments on KC3AC1 cells, a murine CCD cell model revealed the expression of functional GH receptors (GHR) and IGF-1 receptors coupled to activation of JAK2/STAT5, ERK and AKT signaling pathways. That GH directly controls sodium reabsorption in CCD cells is supported by i) stimulation of transepithelial sodium transport inhibited by GHR antagonist pegvisomant ii) induction of αENaC mRNA expression iii) identification of STAT5 binding to a response element located in the αENaC promoter, indicative of the transcriptional regulation of αENaC by GH. Our findings provide first evidence that GH, in concert with IGF-1, stimulates ENaC-mediated sodium transport in the late distal nephron, accounting for the pathogenesis of sodium retention in acromegaly.

Introduction

Chronic hypersecretion of growth hormone (GH) and subsequent hypersecretion of insulin-like growth factor-1 (IGF-1) in acromegaly leads to major cardiovascular complications which constitute the main cause (60%) of mortality. Arterial hypertension that occurs in 30–40% of acromegalic patients is one of the most important prognostic factors of increased mortality (1). Plasma volume expansion and increased cardiac output have been well documented and seem to play major roles in the pathophysiology of high blood pressure (2). In addition, increased extracellular volume is constantly present and accounts for soft-tissue swelling and organomegaly consistent with the antinatriuretic effects of GH (3). In contrast, adult GH-deficient patients have a reduction in plasma and extracellular volume which can be normalized by GH substitution (4). However, the molecular mechanisms by which GH controls sodium and water homeostasis remain poorly understood.

The initial concept of indirect effects of GH via activation of the renin angiotensin aldosterone system (RAAS) (5-8) or decrease of the plasma atrial natriuretic peptide concentration (9-11) is controversial. Rather, several studies concluded to direct stimulatory effects of GH/IGF-1 on renal sodium and water reabsorption (7, 8, 10). Central questions remain whether GH controls tubular sodium transport directly or through its major target IGF-1, and in which segments of the nephron this potential antinatriuretic effect may occur.

The presence of functional GH receptor (GHR) in target cells is a prerequisite for direct renal effects of GH. Indeed, *in situ* hybridization studies in the rat kidney showed that GHR mRNA expression was confined to the proximal tubule and the thick ascending limb of Henle's loop (12). However, the expression of GHR in the distal nephron remains controversial (12-14). Recent observations have extended GHR expression to glomerular mesangial cells (15) and podocytes (16). *In vitro* microperfusion of rabbit proximal tubules exposed to GH and IGF-1 (17) as well as lithium clearance measurements, an important index of proximal tubular sodium reabsorption, in GH-treated patients (10) and rats (18), have excluded a prominent role of the proximal tubule in GH-induced sodium transport. Likewise, although a recent study reported that acute GH administration in rats results in increased phosphorylation of $Na^+,K^+,2Cl^-$ cotransporter (NKCC2) in the thick ascending limb (TAL) of the Henle's loop, the lack of a concomitant GH-induced change in sodium transport questions the physiological relevance of this observation (18). Based on human metabolic studies, it has been alternatively suggested that GH may exert its effects in the distal nephron (8, 10) which plays a pivotal role in sodium homeostasis and constitutes the major segment mediating sodium-retaining effects of the mineralocorticoid hormone aldosterone (19). The classical view of aldosterone action is that it binds to the mineralocorticoid receptor (MR), a ligand-dependent transcription factor, to modulate gene expression, resulting in induction of proteins implicated into the transepithelial ionic transport (20). Aldosterone-regulated transepithelial sodium reabsorption in the distal nephron occurs via the amiloride-sensitive epithelial sodium channel (ENaC) located at the apical membrane and the basolateral Na^+,K^+-ATPase of cortical collecting duct (CDD) cells. ENaC is composed of three subunits (α, β and γ) (21) constituting the rate-limiting step of apical Na^+ entry. Even though the presence of GHR in the distal nephron has been demonstrated in some, but not all studies (12-14), it has thus far never been functionally characterized.

To address the direct impact of GH on the control of sodium handling and to localize its target site of action, we employed complementary approaches on various experimental models which all provided converging evidence for direct antinatriuretic effects of GH in the late distal nephron. Metabolic cage studies in an animal model of acromegaly, the GC rats bearing somatotropic cell tumors (22) allowed us to examine the influence of chronic GH hypersecretion on sodium balance *in vivo* and to identify the aldosterone-sensitive distal nephron as a direct target of GH action. To decipher the mechanisms by which GH stimulated transepithelial sodium transport, we used a highly differentiated cortical collecting duct (CCD) cell line, the KC3AC1 cells (23). This cell-based system enabled us to demonstrate, for the first time, the presence of functional

GHR in a CCD-derived cell line and to characterize the molecular targets involved in the pathophysiology of extracellular volume expansion in acromegaly.

Materials and Methods

Hormones and drugs

GH and pegvisomant were kindly provided by Serono (Boulogne, France) and Pfizer (Paris, France), respectively. IGF-1, U0126 and Ly294002 were from Euromedex (Mundolsheim, France), AG490 was from VWR (Strasbourg, France), protein A sepharose CL-4B was from GE Healthcare (Uppsala, Sweden), and all other reagents were from Sigma-Aldrich (St Louis, MI).

Animal studies

Animal housing and metabolic studies were performed according to the French legislation. GC rats were generated as previously described (22). Briefly, 12 x 10^6 GC cells were injected subcutaneously into the flank of 8-wk-old female Wistar-Furth rats (Charles River, France). Animals were maintained on a regular 12h-light-dark cycle, fed ad libitum, and weighed weekly for 12 weeks. Water intake, baseline 24 h urine volume, urinary creatinine and electrolyte concentrations determined on an automatic analyzer (Konelab 20i, Thermo, Cergy Pontoise, France) were obtained for two consecutive days after three days of animal adaptation to encaging. Furosemide (40 mg/kg) was injected ip and urine was collected during consecutive 3 h urinary sample collections. Amiloride was given in the drinking water (150 mg/L) for 24 h with concomitant 24 h urinary sample collection. Amiloride intake was not different in GC and wild type rats when normalized to body weight (9.8 mg/kg vs 10.2 mg/kg in controls). Plasma GH concentrations were determined by EIA as previously described (24). IGF-1 and aldosterone concentrations were measured by RIA. Three days after metabolic challenges, animals were sacrificed after anesthesia and kidneys were collected for histology and Western blot analysis.

Na^+/K^+-ATP-ase assay

Na^+/K^+-ATP-ase activity was determined using pools of 4-6 permeabilized proximal convoluted tubules, cortical thick ascending limbs of Henle's loop or cortical collecting ducts as described previously (25). Na^+/K^+-ATPase activity was taken as the difference between mean total and ouabain-resistant ATPase activities, each determined in triplicate. Values are means ± SEM from several animals.

Cell culture

KC3AC1 cells (passages 10-20) were seeded on collagen I-coated Transwell filters (Costar Corp. Brumath, France) or Petri dishes and routinely cultured at 37°C in a humidified incubator gassed with 5% CO_2 within an epithelial medium composed of DMEM/HAM's F12 (1:1); 2 mM glutamine; 50 nM dexamethasone; 50 nM sodium selenite; 5 µg/ml transferrin; 5 µg/ml insulin; 10 ng/ml EGF; 2 nM T3; 100 U/ml penicillin, 100 µg/ml streptomycin; 20 mM HEPES, pH 7.4 and 5% dextran charcoal-treated serum (DCC). To study GH actions, epithelial medium was replaced by a minimum medium having the same composition as the epithelial medium with omission of DCC, dexamethasone and EGF. To study IGF-1 effects, insulin was omitted to the minimal medium.

RT-PCR and quantitative real time PCR

Total RNA was extracted from cells with TRIZOL reagent (InVitrogen, Cergy Pontoise, France) and RNA were processed for RT-PCR analysis. Gene expression was quantified by real time PCR, using an ABI 7300 (Applied Biosystems, Foster City, CA). Results represent the relative expression for a given sample calculated as the ratio (amol of specific gene/fmol of 18S). Murine RNAs were extracted from pools of 20-50 microdissected nephronic segments and quantitative real time PCR was performed using a cDNA quantity corresponding to 0.1 mm of nephron. Results are expressed as molecules/mm tubule length. Supplemental Table 1 indicates primer sequences of genes analyzed.

Western blot analysis and immunoprecipitation assay

Total protein extracts were prepared from wild type and GHR knock-out mouse kidney and liver or from KC3AC1 cells. When GH or IGF-1 treatment was tested, cells were deprived for 3 or 24 h in the appropriate minimal media as indicated above. Tissues or cells were washed twice with ice-cold PBS and lysed at 4°C with lysis buffer. Immunoblots

were incubated overnight with following dilutions of primary antibodies: anti-GHR AL-47, 1:1,000 (kindly provided by Pr. SJ. Frank, Birmingham, AL); anti-IGF-1Ra N20: sc-712, 1:1,000, (Santa Cruz Biotechnology Inc., Santa Cruz, CA); anti-phospho-p44/42 MAPK E10, 1:2,000; anti-p44/42 MAPK E10, 1:1,000; anti-phospho-AKT, 1:1,000; anti-AKT, 1:1,000, (all from Cell Signaling Technology Inc, Beverly, MA) and anti-α, β and γEnaC subunits antibodies, 1:1000 (kindly provided by Dr. M. van Bemmelen and Pr. L. Schild, Lausanne, Switzerland) followed by incubation with peroxidase-conjugated goat anti-rabbit antibody, dilution 1:15,000 or anti-mouse antibody, dilution 1:20,000, respectively (Vector, Burlingame, CA) and visualized by the ECL$^+$ detection kit (GE Heathcare). When indicated, immunoprecipitation was performed by incubating 1 mg of total proteins with anti-STAT5 C17 antibody (Santa Cruz) overnight at 4°C and the immunoprecipitates were collected using protein A sepharose CL-4B beads (GE Healthcare), reduced in Laemmli buffer and subjected to 7.5% acrylamide SDS-PAGE and western blot as described above. Electrotransferred proteins were incubated with monoclonal anti-phospho-tyrosine antibody (1:5,000, clone 4G10, Upstate Biotechnology, Lake Placid, NY) followed by incubation with the secondary antibody. For loading normalization, membranes were incubated with anti-STAT5 or anti- α tubulin (1:10,000, DM1A, Sigma). Quantitative analysis of specific signals was performed using Quantity One software (Biorad).

Immunocytochemistry

Cells cultured on Lab-Tek (Nunc), were washed in PBS then fixed with 10% buffered formol in PBS (pH 7.3) for 10 min, washed three times in PBS before processing for immunocytochemistry. Cells cultured on filters were fixed in 10% buffered formol in PBS (pH 7.3) for 60 min, dehydrated and embedded in paraffin blocks. Serial sections were deparaffinized and antigen retrieval was performed in a microwave oven in pH 6 citrate buffer for 15 min. After blocking with 2.5% normal horse serum, cells were incubated overnight with dilution of primary antibodies as follows: anti-GHR AL-47, 1:500; anti-IGF-1Rα, 1:400; anti-phospho-STAT5 sc-11761, 1:200 (Santa Cruz). After endogenous peroxidase quenching, immunodetection was performed using the ImmPress reagent kit (Vector). Irrelevant rabbit immunoglobulins were used as negative controls.

Ionic transport measurements

Cells seeded on collagen I-coated Transwell filters were cultured for 6 days in the epithelial medium which was replaced by the appropriate minimal medium 24 h before hormonal stimulation. The next day, 500 µl of the supernatant were recovered from the medium bathing the apical and basolateral surface of KC3AC1 cells. Ionic concentrations were measured.

EMSA

Differentiated KC3AC1 cells were starved for 3 h in insulin-containing miminal medium and exposed to GH stimulation. Nuclear protein extraction and gel mobility shift assays were performed as described (26). Purified oligonucleotides were annealed and labeled with [^{32}P]-dCTP (GE Healthcare) using the Klenow fragment of DNA polymerase (Life Technologies, Inc., Paisley, UK) to a specific activity of approximately 10^8 cpm/µg of DNA. Oligonucleotide sequences were as follows: αENaC-forward: 5'-GCTTCTCTTCTCGGAACCTCA-3'; αENaC-reverse: 5'-GAAGAGAAGAGCCTTGGAGTG-3'.
Protein-DNA complexes were separated from free DNA by electrophoresis on nondenaturing 4.5% polyacrylamide gel in 0.25X Tris-borate-EDTA buffer at 200 V for 1 h. Gels were dried and exposed to x-ray film at -80°C.

Statistical analysis

Data were analyzed for statistical significance using the software Prism 4 (GraphPad Software, San Diego, CA). We performed either non parametric Mann Whitney test, Kruskal-Wallis multi-variance analysis followed by a post- test analysis of Dunn's comparison test or non parametric Spearman correlation. Levels of statistical significance were fixed for P values < 0.05.

Results

GH enhances sodium transport in the late distal nephron in GC rats

To address the impact of GH hypersecretion on renal electrolyte balance, and to precise the site of altered sodium handling along the nephron,

metabolic studies coupled to pharmacological tests were performed in GC rats, an animal model of acromegaly. After 12 weeks of subcutaneous GC cell implantation leading to chronic GH hypersecretion, GC rats presented with a significant increase in body weight (434.7 ± 16.4 g *vs* 207.0 ± 3.7 g for wild-type (WT) animals, $P<0.001$), consistent with the very high GH concentrations in GC rats as compared with control group (WT 10.0 ± 1.4 ng/mL and GC 8217.0 ± 1088.2 ng/mL, $P<0.01$). As expected, this was also accompanied by a signifiant increase in IGF-1 levels (WT 395 ± 38 ng/mL and GC 1707 ± 146 ng/mL, $P<0.001$). Interestingly, we constantly observed a dramatic 3.5-fold renal hypertrophy leading to a 1.6-fold increase in kidney weight/body weight ratio in acromegalic animals, suggesting a specific impact of chronic GH hypersecretion on kidney remodeling (Fig. 1A and 1B). In addition, histological examination disclosed a major interstitial oedema associated with a 1.7-fold increase in glomerular size (WT 89.9 ± 3.2 *vs* GC 155.9 ± 3.5 µm, $P<0.01$). Despite this glomerular hypertrophy which paralleled the renal hypertrophy, we did not observe any modification in the diameter of the microdissected cortical collecting ducts of the acromegalic animals (Fig. 1D).

As shown in Fig. 2A and B, basal Na^+ and K^+ excretion did not differ in wild type (WT) and GC rats. Administration of furosemide, an inhibitor of the $Na^+/K^+/2Cl^-$ cotransporter, led to lower natriuretic responses and lower urinary Na^+/K^+ ratio in GC compared to WT rats (Fig. 2A). Given that furosemide increased luminal Na^+ delivery downstream of the Henle's loop, this difference might be accounted for by enhanced sodium reabsorption in the distal parts of the nephron. This hypothesis was validated by showing that the natriuretic response to amiloride, a potent inhibitor of ENaC, was enhanced 1.5-fold in GC rats, and was associated with decreased kaliuresis (urinary Na^+/K^+ ratio increased 3.8-fold *vs* WT) (Fig. 2B). We clearly demonstrated an enhanced capacity of the late distal nephron of GC rats to reabsorb Na^+ and secrete K^+, in spite of a significant reduction in plasma aldosterone concentrations in GC rat compared to controls (Fig 2.C). We next measured the Na^+/K^+-ATP-ase activity, the motor of sodium reabsorption along the nephron, in discrete nephron segments and showed that the Na^+/K^+-ATP-ase activity was specifically increased in the CCD of GC rats whereas it was not altered in the proximal tubule (PCT) and the Henle's loop (cTAL) (Fig. 2D). Taken together, these *in vivo* studies provide direct evidence that chronic GH/IGF-1 excess enhances sodium transport in the late distal nephron in acromegaly, independently of the renin-angiotensin-aldosterone system.

Chronic GH excess enhances ENaC maturation by proteolytic cleavage of α and γ subunits

Since sodium reabsorption in the aldosterone-sensitive distal nephron is mainly mediated by ENaC, we examined the renal expression of its three subunits by Western blot analysis in the GC and WT rats. Fig. 3A shows unchanged expression of the 95-kDa and 55-kDa forms of α subunit but a distinct electrophoretic pattern of lower molecular mass bands observed in GC rats. Indeed, the expression of the 36-kDa fragment was decreased in GC rats, associated with a shift of the 38- to a 40-kDa band (Fig.3A , arrowhead). The expression of the 100-110 kDa forms of the β subunit of ENaC remained unchanged (Fig. 3B). Furthermore, the abundance of the 85-kDa and 75-kDa forms of the γ subunit was not altered. Strikingly, an intermediate ~80-kDa fragment clearly appeared in GC rats compared to controls (Fig. 3C; arrowhead). Altogether, these results demonstrate that enhanced sodium transport prevailing in the distal nephron of GC rats correlates with a significant modification of ENaC maturation involving distinct proteolytic processing of the α and γ subunits.

GHR and IGF-1R are expressed in cortical collecting duct cells

To establish whether GH exerts direct effects in the distal parts of the nephron, we first analyzed the expression profile of GHR (left panel) and IGF-1R (right panel) mRNA on microdissected murine nephronic segments by quantitative real-time PCR (Fig. 4A). Beside the well-described expression of GHR and IGF-1R mRNAs in the proximal tubule and Henle's loop, we detected substantial amounts of GHR and IGF-1R in the distal nephron with an expression gradient from the cortex to the medulla. To further investigate the molecular mechanisms involved in the antinatriuretic

effects of GH and/or IGF-1 in the CCD, we used the KC3AC1 cells which maintain aldosterone responsiveness and functional mineralocorticoid receptor signaling (23). When cultured on collagen-coated Petri dishes, KC3AC1 cells develop at confluence numerous domes, a characteristic morphological feature of highly differentiated polarized epithelial cells (Fig. 4B). The relative abundance of GHR and IGF-1R mRNA in undifferentiated and fully differentiated dome-forming cells was measured by quantitative real-time PCR and compared to that determined in microdissected murine CCD. We showed that the levels of receptor transcripts increase as a function of the cell differentiation (Fig. 4C) and the relative GHR transcript abundance in KC3AC1 cells was comparable to that of endogenous GHR expressed in isolated cortical collecting ducts, estimated at approx 0.25 amol/µg RNA or 10,000 molecules /µg of cellular proteins. Western blot analysis using anti-GHR AL47 antibody revealed a specific band migrating at 115 kDa in KC3AC1 whole-cell lysates, also present in murine kidney and liver protein extracts. In contrast, it was absent in GHR knock-out mouse organs in which only the 82 kDa non-specific bands were detected, thus confirming the specificity of the higher molecular weight band (Fig. 4D). These results are consistent with the presence of the GHR protein in KC3AC1 cells. IGF-1R protein expression was also analyzed by Western blot. Fig. 4E reveals two specific bands migrating at 130 kDa and 200 kDa in KC3AC1 cell lysates and in murine kidney, providing evidence for the presence of the α subunit of IGF-1R protein. GHR and IGF-1R protein expression in KC3AC1 cells was further analyzed by immunocytochemistry. Fig. 4F and 4G illustrate GHR and IGF-1R immunostainings in KC3AC1 grown on Petri dishes, as well as in a monolayer of KC3AC1 cells cultured on filters. The GHR and IGF-1R immunoreactivity was predominantly localized to the cell membrane and the adjacent cytoplasm and was enhanced in the dome areas. Finally, KC3AC1 cells did not express IGF-1 either in basal conditions or after GH stimulation (data not shown). Collectively, these results demonstrate conclusively that KC3AC1 cells express GHR and IGF-1R both at mRNA and protein level but not IGF-1 enabling us to distinguish direct GH-induced effects from those mediated via IGF-1.

GHR and IGF-1R signaling in KC3AC1 cells

To assess the functional integrity of GHR in KC3AC1 cells, we examined the activation of the classical GHR-associated signaling pathways. GH treatment led to a rapid STAT5 phosphorylation visible as early as 5 min and sustained until 60 min after hormonal stimulation (Fig. 5A). This dose-dependent effect was maximal at a GH concentration of 1000 ng/ml and was strongly antagonized (70%) by the JAK2 inhibitor AG490 and partially inhibited (40%) by the GHR antagonist pegvisomant as determined by image density quantification (Fig. 5B). Immunocytochemistry with an antiphospho-STAT5 antibody showed a transient nuclear translocation of phosphorylated STAT5 in KC3AC1 cells 30 min after GH stimulation (Fig. 5C). GH exposure also induced a rapid and transient ERK1/2 phosphorylation with the maximal response 2 min after stimulation (Fig. 5D). This effect was completely inhibited by the GHR antagonist pegvisomant and the MEK inhibitor U0126 (Fig. 5E). The IGF-1R signaling in KC3AC1 cells was also examined by activation of its canonical signaling pathways. As shown by western blot analysis, IGF-1 treatment at a concentration of 10 nM resulted in rapid and transient ERK1/2 phosphorylation with maximal response 2 min after hormonal stimulation (Fig. 5F) and prolonged AKT phosphorylation lasting 5–30 min (Fig. 5G). Full inhibition of these effects by the respective kinase inhibitors U0126 and Ly294002 proved the specificity of the IGF-1R signaling. Taken together, these studies provide strong evidence for the functional integrity of the GHR and IGF-1R signaling in KC3AC1 cells, thus constituting a suitable cell-based system to study biological effects of GH and IGF-1 in the CCD.

GH and IGF-1 stimulate ionic transports in KC3AC1 cells

To investigate the potential impact of GH and IGF-1 on ionic transport in CCD cells, we used KC3AC1 cells cultured on Transwell filters that exhibited a high transpithelial resistance (5.27 ± 0.17 KΩ/cm^2) and an amiloride-sensitive short-circuit current (Isc) 23.95 ± 5.27 µA consistent with an ENaC-dependent sodium transport (23). Ion concentrations in

the apical and basolateral compartments were measured after GH exposure (100 ng/ml). Under basal conditions, KC3AC1 cells generated apical to basolateral Na^+ and Cl^- gradients (Na^+ : 4.40 ± 0.61 and Cl^- : 3.60 ± 0.34 mmol/ml/24 h) indicating a Na^+/Cl^- reabsorption, accompanied by a K^+ secretion with basolateral to apical gradient of 1.22 ± 0.21 mmol/ml/24h. GH treatment (100 ng/ml) induced a 60% increase in Na^+ reabsorption and comparable increase in Cl^- reabsorption (Fig. 6A and C). The effects were completely inhibited by the GHR antagonist pegvisomant, establishing unambiguously the involvement of GH/GHR activation cascade. Of note, GH did not significantly influence potassium transport under these experimental conditions (Fig. 6B). On the other hand, IGF-1 (10 nM) induced a 100 % increase in Na^+ with a 50% increase in Cl^- transepithelial gradient. Importantly, it was accompanied by a sharp 3.5-fold increase in K^+ transepithelial gradient (Fig. 6D–F). These findings demonstrate that GH exerts direct stimulatory effects on Na^+ and Cl^- reabsorption in CCD-derived cells, while IGF-1 induces Na^+/Cl^- reabsorption with a marked K^+ secretion.

αENaC is a direct GH target gene in cortical collecting duct cells

To decipher the molecular bases of the GH-induced increase in Na^+ reabsorption, gene expression analyses were performed by quantitative real-time PCR experiments on GH-treated KC3AC1 cells. We first demonstrated that GH induced a 2 to 3-fold increase in the expression of SOCS2 and CIS, two classical GH target genes (Fig. 7A, upper and middle panels). GH exposure also led to a significant 30% increase in αENAC but not βENAC and γENAC mRNA steady state levels, suggesting that αENAC is a novel renal target of GH (Fig. 7A, lower panel). Since GH treatment of KC3AC1 cells induced STAT5 phosphorylation (see Fig. 5A-C), we analyzed the promoter sequence of *SCNN1A* and identified a perfectly conserved STAT5 response element located -2097 bp upstream of the transcription initiation start site of the gene. As shown in Fig. 7B, electromobility shift assays with nuclear proteins extracted from untreated or GH-treated KC3AC1 cells demonstrated the presence of specific STAT5-RE-protein complexes in GH-treated extracts, suggesting that GH regulates *αENaC* transcription via STAT5 activation. Collectively, our results clearly demonstrate that αENaC expression is directly stimulated by acute exposure to GH, a finding consistent with the enhanced capacity of CCD cells to reabsorb sodium accounting for hydroelectrolytic retention observed in acromegaly. Since IGF-1 also regulated transepithelial ionic transport in this cell model, we examined the putative transcriptional control of IGF-1 on candidate target gene expression. At variance with GH, αENAC mRNA expression was not affected whereas the expression of Sgk1 transcripts was rapidly and transiently stimulated as early as 30 min after IGF-1 exposure (Fig. 7C). Sgk1 expression was not modified by GH treatment (data not shown). Taken together, we demonstrated that GH and IGF-1 modulate distinct target genes implicated in the regulation of ionic transport in the CCD cells, a finding suggesting that both hormones could cooperate to control sodium balance.

Discussion

Even though the antinatriuretic effects of GH have been proposed long time ago (3), the mechanisms by which GH and/or IGF-1 regulate sodium and water balance remain poorly understood. In the present study, several lines of evidence indicate direct antinatriuretic effects of GH in the late distal nephron. We demonstrate that acromegaly leads to enhanced amiloride-sensitive sodium transport in the CCD associated with GH-induced transcriptional activation and proteolytic maturation of ENaC.

Renal metabolic studies in GC rats permitted to exclude a major contribution of Henle's loop in sodium retaining effects of GH excess. Instead the increase in amiloride-stimulated natriuresis and the decrease in furosemide-induced natriuresis together with the specific increase in Na^+/K^+-ATP-ase activity in CCD clearly revealed the pivotal role of the distal nephron as the major site of GH/IGF-1 induced sodium retention in acromegaly. Of interest, six weeks after tumor removal in GC rats with normal circulating GH concentrations, the natriuretic responses to furosemide and amiloride challenge returned to the normal ranges (data not shown), indicating that chronic GH and/or IGF-1 exposure are indeed responsible for altered Na^+ excretion.

However, these functional renal investigations do not permit to precise the relative contribution of GH and IGF-1 to the increased sodium transport prevailing in the CCD. Considering the distinct half-lives of GH (18 min) and IGF-1 (8-9 h) (27, 28), the massive polyuria and dramatic tissue swelling regression generally observed few hours after pituitary tumor removal in acromegalic patients support a direct and rapid control of renal sodium reabsorption by GH. Since GH concentrations in GC rats are about two orders of magnitude higher than those measured in acromegalic patients, one has to be caution when translating these observations to human pathology.

The molecular mechanisms by which GH exerts its antinatriuretic effects are not entirely clear. The major effect of amiloride on sodium excretion demonstrated in GC rats points out to a prominent role played by ENaC as the key mediator of GH action. Here, we show that chronic GH excess leads to major modifications in the proteolytic maturation of both α and γ subunits of ENaC in GC rat kidneys. Indeed, proteolytic cleavage of α and γ ENaC subunits by furin, a serine protease, is associated with increased channel activity (29, 30). Recent studies suggested, that a second cleavage event within the γ ENaC subunit, by prostasin (31) or by neutrophil elastase (32), releasing an inhibitory peptide domain, was required to fully activate the channel (33). Along this line, the intermediate 80-kDa γ ENaC band observed in GC rats could represent an increased pool of furin-cleaved γ subunit. Finally, ENaC processing in the kidney is regulated by distinct physiological or pathological stimuli including hyperaldosteronism due to either sodium restriction or aldosterone administration (34, 35). However, increased sodium reabsorption in the CCD accompanied by ENaC proteolytic maturation despite low plasma aldosterone concentrations in acromegalic rats provide additional evidence that GH/IGF-1 directly control ENaC activity, irrespective of the mineralocorticoid status.

To gain more insight into the molecular events underlying GH-induced regulation of sodium reabsorption in the distal nephron, we employed the renal KC3AC1 cell line. To the best of our knowledge, our study is the first report demonstrating functional GHR expression in CCD-derived cells, the site of the aldosterone-sensitive sodium transport (36). In addition, since KC3AC1 cells did express functional IGF-1R but not IGF-1, this cell based system also enabled us to directly assess the impact of IGF-1 actions on CCD cells, independently from those induced by GH. As expected, GH treatment of KC3AC1 cells resulted in activation of canonical JAK2/STAT5 and ERK1/2 signaling pathways (37) and in the induction of classical GH target genes such as *SOCS2* and *CIS* (38, 39). One of the main findings is that GH also exerts direct stimulatory effects on transcriptional regulation of *αENaC* expression. This effect appears to be linked to JAK2/STAT5 activation, as we have identified a STAT5 response element in the promoter of *SCNN1A* gene conserved in mice, rats and humans. Since a cross-talk between cytokine receptor signaling pathways and steroid receptors has been already documented (40), a functional link between mineralocorticoid receptor (MR), the key transcriptional regulator in CDD cells, and STAT5 is very likely given the vicinity of their respective response elements on the *SCNN1A* promoter. Whether MR and STAT5 physically interact and how they functionally cooperate to activate transcription remains to be addressed experimentally.

Our study conclusively demonstrates that GH exposure not only stimulates transcription of *α*ENaC but also affects ENaC subunits proteolytic maturation. Considering that ENaC activity depends on other complex regulatory mechanisms including post-transcriptional regulation by Nedd4-2-mediated ubiquitinylation that controls apical membrane abundance as well as alteration of the open probability (P_o) of functional channels (34, 36, 41), it remains to investigate whether the antinatriuretic effects of GH may also involve modification in the residency time and functional properties of the apical channels.

From a physiological perspective, it is interesting to note that lactogens and GH signaling play essential role in the osmoregulation and in the salinity adaptation of teleost fishes (42, 43). Consistent with our finding, a recent study suggests that prolactin induces sodium transport via stimulation of ENaC and Na^+/K^+-pump activities in the amphibian skin (44). Lactogen/GH-dependent ENaC activation could represent an important phylogenetic axis in the control of the “milieu

intérieur" conserved throughout hundreds millions of years of evolution.

Beside GH, IGF-1 also stimulates transepithelial sodium transport, in accordance with previous studies on other mammalian and amphibian cell lines (45-48). It has been proposed that, like insulin (49), IGF-1 controls sodium transport via increase in Sgk1 protein level and PI-3K-mediated Sgk1 phosphorylation (48), leading to subsequent inactivation of the ubiquitin ligase Nedd4-2 (41). Here, we provide first evidence that IGF-1 also regulates *Sgk1* transcription which, together with its well-known aldosterone dependent induction (50), represents an additional cross-talk bewteen aldosterone and IGF-1 signaling pathway.

Based on our results, we propose a model of cooperative GH and IGF-1 action in CCD cells leading to an intricate control of transepithelial sodium reabsorption that is schematized in Figure 8. GH binding to GHR triggers activation of JAK2/STAT5 and MAP kinase pathways, leading to transcriptional activation of the classical and kidney-specific GH target genes including *αENaC*. ENaC activity is also modulated by post-transcriptional and post-translational events including proteolytic maturation of α and γ subunits. IGF-1, locally synthesized in the kidney or produced in the liver, binds to IGF-1R and regulates apical membrane abundance of ENaC via PI-3K-dependent Sgk1 activation (47, 48).

In summary, our findings reveal the critical role of GHR signaling in sodium transport of CCD cells. The demonstration of a direct GH action mediated by ENaC activation provides a novel mechanism which, in concert with IGF-1, accounts for the regulation of sodium homeostasis. Given the importance of sodium balance in the pathogenesis of arterial hypertension, our study opens new therapeutic strategies to prevent or cure cardiovascular complications in acromegalic patients.

Acknowledgments

The authors are indebted to Pr. Stuart Frank (University of Alabama, Birmingham, AL) for his gift of anti-GHR AL-47 antibody and helpful advices for immunodetection assays, to Dr. Miguel van Bemmelen and Pr. Laurent Schild, (University of Lausanne, Switzerland) for their gifts of anti-ENaC antibodies and to Pr. John Kopchick (Ohio University, Athens, OH) for his permission to use GHR knockout mice, to Dr. Marie-Thérèse Bluet-Pajot (Inserm U 549, Paris, France) for her assistance in the initial investigation of GC rats, to Dr. Nadine Binart (Inserm U 845, Paris, France) for critical and helpful discussions. The assistance of Dr Anne Davit-Spraul (Department of Biochemistry, Hôpital de Bicêtre) for ionic measurements, of Annick Ganieux (IFR 93 Bicêtre) for plasmid preparation and of Roman Bogorad (Inserm U 845, Paris, France) for immunoprecipitation assays is also gratefully acknowledged. This work was supported by fundings from Inserm and Université Paris-Sud 11, and a grant from Pfizer, France. PK was a recipient of fellowship from the Gouvernement Français (Egide) and from the Ministère de l'Enseignement Supérieur et de la Recherche, France.

References

1. **Melmed S** 2006 Medical progress: Acromegaly. N Engl J Med 355:2558-2573
2. **Chanson P, Timsit J, Masquet C, Warnet A, Guillausseau PJ, Birman P, Harris AG, Lubetzki J** 1990 Cardiovascular effects of the somatostatin analog octreotide in acromegaly. Ann Intern Med 113:921-925
3. **Ikkos D, Luft R, Sjogren B** 1954 Body water and sodium in patients with acromegaly. J Clin Invest 33:989-994
4. **Amato G, Carella C, Fazio S, La Montagna G, Cittadini A, Sabatini D, Marciano-Mone C, Sacca L, Bellastella A** 1993 Body composition, bone metabolism, and heart structure and function in growth hormone (GH)-deficient adults before and after GH replacement therapy at low doses. J Clin Endocrinol Metab 77:1671-1676
5. **Ho KY, Weissberger AJ** 1990 The antinatriuretic action of biosynthetic human growth hormone in man involves activation of the renin-angiotensin system. Metabolism 39:133-137
6. **Hoffman DM, Crampton L, Sernia C, Nguyen TV, Ho KK** 1996 Short-term growth hormone (GH) treatment of GH-deficient adults increases body sodium and extracellular water, but not blood pressure. J Clin Endocrinol Metab 81:1123-1128
7. **Hayes FJ, Fiad TM, McKenna TJ** 1997 Activity of the renin-angiotensin-aldosterone axis is dependent on the occurrence of edema in growth hormone (GH)-deficient adults treated with GH. J Clin Endocrinol Metab 82:322-323
8. **Hansen TK, Moller J, Thomsen K, Frandsen E, Dall R, Jorgensen JO, Christiansen JS** 2001 Effects of growth hormone on renal tubular handling of sodium in healthy humans. Am J Physiol Endocrinol Metab 281:E1326-1332
9. **Moller J, Jorgensen JO, Moller N, Hansen KW, Pedersen EB, Christiansen JS** 1991 Expansion of extracellular volume and suppression of atrial natriuretic peptide after growth hormone administration in normal man. J Clin Endocrinol Metab 72:768-772
10. **Johannsson G, Sverrisdottir YB, Ellegard L, Lundberg PA, Herlitz H** 2002 GH increases extracellular volume by stimulating sodium reabsorption in the distal nephron and preventing pressure natriuresis. J Clin Endocrinol Metab 87:1743-1749
11. **Johannsson G, Gibney J, Wolthers T, Leung KC, Ho KK** 2005 Independent and combined effects of testosterone and growth hormone on extracellular water in hypopituitary men. J Clin Endocrinol Metab 90:3989-3994
12. **Chin E, Zhou J, Bondy CA** 1992 Renal growth hormone receptor gene expression: relationship to renal insulin-like growth factor system. Endocrinology 131:3061-3066
13. **Lobie PE, Garcia-Aragon J, Wang BS, Baumbach WR, Waters MJ** 1992 Cellular localization of the growth hormone binding protein in the rat. Endocrinology 130:3057-3065
14. **Mertani HC, Morel G** 1995 In situ gene expression of growth hormone (GH) receptor and GH binding protein in adult male rat tissues. Mol Cell Endocrinol 109:47-61
15. **Doi SQ, Jacot TA, Sellitti DF, Hirszel P, Hirata MH, Striker GE, Striker LJ** 2000 Growth hormone increases inducible nitric oxide synthase expression in mesangial cells. J Am Soc Nephrol 11:1419-1425
16. **Reddy GR, Pushpanathan MJ, Ransom RF, Holzman LB, Brosius FC, 3rd, Diakonova M, Mathieson P, Saleem MA, List EO, Kopchick JJ, Frank SJ, Menon RK** 2007 Identification of the glomerular podocyte as a target for growth hormone action. Endocrinology 148:2045-2055
17. **Quigley R, Baum M** 1991 Effects of growth hormone and insulin-like growth factor I on rabbit proximal convoluted tubule transport. J Clin Invest 88:368-374
18. **Dimke H, Flyvbjerg A, Bourgeois S, Thomsen K, Frokiaer J, Houillier P, Nielsen S, Frische S** 2007 Acute growth hormone administration induces antidiuretic and antinatriuretic effects and increases phosphorylation of NKCC2. Am J Physiol Renal Physiol 292:F723-735
19. **Fuller PJ, Young MJ** 2005 Mechanisms of mineralocorticoid action. Hypertension 46:1227-1235
20. **Viengchareun S, Le Menuet D, Martinerie L, Munier M, Pascual-Le Tallec P, Lombes M** 2007 The mineralocortcioid receptor: insights in its molecular and (patho)physiological biology. Nucl Rec Signal 5:e012

21. **Canessa CM, Schild L, Buell G, Thorens B, Gautschi I, Horisberger JD, Rossier BC** 1994 Amiloride-sensitive epithelial Na+ channel is made of three homologous subunits. Nature 367:463-467
22. **Timsit J, Riou B, Bertherat J, Wisnewsky C, Kato NS, Weisberg AS, Lubetzki J, Lecarpentier Y, Winegrad S, Mercadier JJ** 1990 Effects of chronic growth hormone hypersecretion on intrinsic contractility, energetics, isomyosin pattern, and myosin adenosine triphosphatase activity of rat left ventricle. J Clin Invest 86:507-515
23. **Le Menuet D, Viengchareun S, Muffat-Joly M, Zennaro MC, Lombes M** 2004 Expression and function of the human mineralocorticoid receptor: lessons from transgenic mouse models. Mol Cell Endocrinol 217:127-136
24. **Ezan E, Laplante E, Bluet-Pajot MT, Mounier F, Mamas S, Grouselle D, Grognet JM, Kordon C** 1997 An enzyme immunoassay for rat growth hormone: validation and application to the determination of plasma levels and in vitro release. J Immunoassay 18:335-356
25. **Deschenes G, Doucet A** 2000 Collecting duct (Na+/K+)-ATPase activity is correlated with urinary sodium excretion in rat nephrotic syndromes. J Am Soc Nephrol 11:604-615
26. **Lombes M, Binart N, Oblin ME, Joulin V, Baulieu EE** 1993 Characterization of the interaction of the human mineralocorticosteroid receptor with hormone response elements. Biochem J 292 (Pt 2):577-583
27. **Peacey SR, Toogood AA, Veldhuis JD, Thorner MO, Shalet SM** 2001 The relationship between 24-hour growth hormone secretion and insulin-like growth factor I in patients with successfully treated acromegaly: impact of surgery or radiotherapy. J Clin Endocrinol Metab 86:259-266
28. **Vaccarello MA, Diamond FB, Jr., Guevara-Aguirre J, Rosenbloom AL, Fielder PJ, Gargosky S, Cohen P, Wilson K, Rosenfeld RG** 1993 Hormonal and metabolic effects and pharmacokinetics of recombinant insulin-like growth factor-I in growth hormone receptor deficiency/Laron syndrome. J Clin Endocrinol Metab 77:273-280
29. **Hughey RP, Mueller GM, Bruns JB, Kinlough CL, Poland PA, Harkleroad KL, Carattino MD, Kleyman TR** 2003 Maturation of the epithelial Na+ channel involves proteolytic processing of the alpha- and gamma-subunits. J Biol Chem 278:37073-37082
30. **Hughey RP, Bruns JB, Kinlough CL, Harkleroad KL, Tong Q, Carattino MD, Johnson JP, Stockand JD, Kleyman TR** 2004 Epithelial sodium channels are activated by furin-dependent proteolysis. J Biol Chem 279:18111-18114
31. **Bruns JB, Carattino MD, Sheng S, Maarouf AB, Weisz OA, Pilewski JM, Hughey RP, Kleyman TR** 2007 Epithelial Na+ channels are fully activated by furin- and prostasin-dependent release of an inhibitory peptide from the gamma-subunit. J Biol Chem 282:6153-6160
32. **Harris M, Firsov D, Vuagniaux G, Stutts MJ, Rossier BC** 2007 A novel neutrophil elastase inhibitor prevents elastase activation and surface cleavage of the epithelial sodium channel expressed in Xenopus laevis oocytes. J Biol Chem 282:58-64
33. **Hughey RP, Carattino MD, Kleyman TR** 2007 Role of proteolysis in the activation of epithelial sodium channels. Curr Opin Nephrol Hypertens 16:444-450
34. **Masilamani S, Kim GH, Mitchell C, Wade JB, Knepper MA** 1999 Aldosterone-mediated regulation of ENaC alpha, beta, and gamma subunit proteins in rat kidney. J Clin Invest 104:R19-23
35. **Ergonul Z, Frindt G, Palmer LG** 2006 Regulation of maturation and processing of ENaC subunits in the rat kidney. Am J Physiol Renal Physiol 291:F683-693
36. **Rossier BC, Pradervand S, Schild L, Hummler E** 2002 Epithelial sodium channel and the control of sodium balance: interaction between genetic and environmental factors. Annu Rev Physiol 64:877-897
37. **Herrington J, Smit LS, Schwartz J, Carter-Su C** 2000 The role of STAT proteins in growth hormone signaling. Oncogene 19:2585-2597
38. **Greenhalgh CJ, Rico-Bautista E, Lorentzon M, Thaus AL, Morgan PO, Willson TA, Zervoudakis P, Metcalf D, Street I, Nicola NA, Nash AD, Fabri LJ, Norstedt G, Ohlsson C, Flores-Morales A, Alexander WS, Hilton DJ** 2005 SOCS2 negatively regulates growth hormone action in vitro and in vivo. J Clin Invest 115:397-406

39. **Endo TA, Masuhara M, Yokouchi M, Suzuki R, Sakamoto H, Mitsui K, Matsumoto A, Tanimura S, Ohtsubo M, Misawa H, Miyazaki T, Leonor N, Taniguchi T, Fujita T, Kanakura Y, Komiya S, Yoshimura A** 1997 A new protein containing an SH2 domain that inhibits JAK kinases. Nature 387:921-924
40. **Stocklin E, Wissler M, Gouilleux F, Groner B** 1996 Functional interactions between Stat5 and the glucocorticoid receptor. Nature 383:726-728
41. **Debonneville C, Flores SY, Kamynina E, Plant PJ, Tauxe C, Thomas MA, Munster C, Chraibi A, Pratt JH, Horisberger JD, Pearce D, Loffing J, Staub O** 2001 Phosphorylation of Nedd4-2 by Sgk1 regulates epithelial Na(+) channel cell surface expression. Embo J 20:7052-7059
42. **Liu NA, Liu Q, Wawrowsky K, Yang Z, Lin S, Melmed S** 2006 Prolactin receptor signaling mediates the osmotic response of embryonic zebrafish lactotrophs. Mol Endocrinol 20:871-880
43. **Sakamoto T, McCormick SD** 2006 Prolactin and growth hormone in fish osmoregulation. Gen Comp Endocrinol 147:24-30
44. **Takada M, Hokari S** 2007 Prolactin increases Na+ transport across adult bullfrog skin via stimulation of both ENaC and Na+/K+-pump. Gen Comp Endocrinol 151:325-331
45. **Blazer-Yost BL, Cox M, Furlanetto R** 1989 Insulin and IGF I receptor-mediated Na+ transport in toad urinary bladders. Am J Physiol 257:C612-620
46. **Matsumoto PS, Ohara A, Duchatelle P, Eaton DC** 1993 Tyrosine kinase regulates epithelial sodium transport in A6 cells. Am J Physiol 264:C246-250
47. **Staruschenko A, Pochynyuk O, Vandewalle A, Bugaj V, Stockand JD** 2007 Acute Regulation of the Epithelial Na+ Channel by Phosphatidylinositide 3-OH Kinase Signaling in Native Collecting Duct Principal Cells. J Am Soc Nephrol 18:1652-1661
48. **Gonzalez-Rodriguez E, Gaeggeler HP, Rossier BC** 2007 IGF-1 vs insulin: respective roles in modulating sodium transport via the PI-3 kinase/Sgk1 pathway in a cortical collecting duct cell line. Kidney Int 71:116-125
49. **Wang J, Barbry P, Maiyar AC, Rozansky DJ, Bhargava A, Leong M, Firestone GL, Pearce D** 2001 SGK integrates insulin and mineralocorticoid regulation of epithelial sodium transport. Am J Physiol Renal Physiol 280:F303-313
50. **Chen SY, Bhargava A, Mastroberardino L, Meijer OC, Wang J, Buse P, Firestone GL, Verrey F, Pearce D** 1999 Epithelial sodium channel regulated by aldosterone-induced protein sgk. Proc Natl Acad Sci U S A 96:2514-2519

Figure Legends

Figure 1: Renal hypertrophy in GC rats is not accompanied by modification of tubular diameter. **A)** Morphologic features of wild type (WT) and GC rat kidney; the scale is in mm. **B)** Comparison of kidney weight (left panel) and kidney weight/body weight ratio (right panel) in WT and GC rats; body weight of WT rats was 207 ± 3.7 g and of GC rats was 434.7 ± 16.4 g. (mean ± SEM , n=10 ; ** $P<0.01$). **C)** Histological features of WT and GC rat kidneys (Magnification x10, bar = 100 μm) **D)** Representative microdissected CCD of WT and GC rats (Magnification x 2.5 , bar = 100 μm).

Figure 2: The amiloride-sensitive distal nephron is the site of enhanced sodium transport in GC rats independently of aldosterone action
A-B) Metabolic studies of renal Na^+ and K^+ handling in basal conditions, and 3 h after furosemide injection (40 mg/kg) (A) and 24 h after oral amiloride administration (150 mg/L of water) (B). Left panels represent basal and furosemide- (A) or amiloride- (B) induced natriuresis normalized by urinary creatinine in WT (□) and GC (■) rats; right panels show urinary Na^+/K^+ ratio in the same experiments. Data are expressed as mean ± SEM, n=10 (** $P<0.01$, *** $P<0.001$).
C) Plasma aldosterone concentrations in WT and GC rats. Values are means ± SEM, from 8 control and 6 GC rats, ** $P< 0.01$
D) Na^+/K^+-ATP-ase activity in proximal convoluted tubule (PCT), cortical thick ascending limb of the Henle's loop (cTAL) and CCD from WT and GC rats. Values (in pmol/mm/h) are means ± SEM from 5 controls and 6 GC rats; *** $P< 0.001$.

Figure 3: ENaC subunits expression and processing is altered in GC rats
A (α subunit)**, B** (β subunit)**,** and **C** (γ subunit)**:** Representative immunoblots of WT (the first three lanes) and GC rat (the last four lanes) kidneys. Twenty micrograms of protein from whole kidney homogenates were loaded onto each lane. Immunoblots were incubated with 1 :1000 dilutions of anti-α, β and γENaC antibodies. Protein loadings were normalized by reblotting with anti-α-tubulin antibody.

Figure 4: GHR and IGF-1R are expressed in KC3AC1 cells
A) Relative GHR and IGF-1R expression along different segments of the mouse nephron was evaluated by quantitative real time PCR. PCT: proximal convoluted tubule; PST: proximal straight tubule; mTAL, cTAL: medullary, cortical thick ascending limb of the Henle's loop; DCT: distal convoluted tubule; CNT: connecting segment; CCD: cortical collecting duct; OMCD: outer medulla collecting duct. Results (molecule/mm tubule length) are expressed as means ± SEM from 5 mice. Note that the scale for GHR expression in PCT and PST (white bars) is ten times higher than that for the other tubular segments (black bars).
B) Morphologic features of subconfluent (left panel) and differentiated dome-forming (right panel) KC3AC1 cells on phase-contrast micrographs (magnification x 20).
C) GHR and IGF-1R mRNA expression in undifferentiated and differentiated KC3AC1 cells were quantified by quantitative real time PCR analysis. A 2.5-fold increase in GHR transcript levels was observed in dome-forming cells as compared to undifferentiated cells whereas IGF-1R expression was only increased by 50%. Results are mean ± SEM of at least 9 independent determinations and represent fold induction above basal expression which was 0.091 ± 0.015 and 0.305 ± 0.046 amol /fmol of 18S for GHR and IGF-1R, respectively (*** $p<0.001$, ** $p<0.01$).
D and E) Western blot analysis of GHR (D) and IGF-1Rα (E) expression in KC3AC1 cells. Thirty μg of proteins from KC3AC1 cell homogenates, wild-type (WT) and GHR KO kidney and liver were processed for immunoblotting with anti-GHR. Note the presence of a specific 115 kDa band for GHR in KC3AC1 cells. Ten or 50 μg of proteins extracted from KC3AC1 cells or whole kidney, respectively, were used for IGF-1R detection which revealed a 200 kDa and a 130 kDa specific band for IGF-1R.
F and G) Immunocytochemical detection of GHR (F) and IGF-1R (G) in dome-forming cells (upper panels) and cells cultured on filters (lower panels).

Figure 5: GHR and IGF-1R signaling in KC3AC1 cells
A and B) KC3AC1 cells were stimulated with 1000 ng/ml GH for 0 to 60 min (A) or increasing concentrations of GH for 15 min (B) or with 10 µg/ml pegvisomant (Peg) or 10 µM AG490 alone (-) or in the presence of 1000 ng/ml GH (+ GH). Lysates were prepared at indicated time and 1 mg proteins were immunoprecipitated (IP) with anti-STAT5 antibody followed by western blotting (WB) using anti-phospho-tyrosine antibody. Membranes were reblotted with anti-STAT5 antibody for loading control.
C) KC3AC1 cells grown on Lab-Tek were incubated or not with 100 ng/ml GH for 15 min. Immunocytochemistry with an anti-phospho-STAT5 antibody revealed a specific nuclear staining in the GH-treated cells (see inset).
D and E) For ERK1/2 pathway, cells were treated with 1000 ng/ml GH for 0-30 min and direct WB on 30 µg protein lysates was performed with anti-phospho-p44/42 antibody (D). Similar experiments were performed in the absence or presence of 1000 ng/ml GH alone or with 10 µg/ml Peg or 10 µM U_{0126} for 2 min (E). Protein loadings were normalized by reblotting with anti-p44/p42 antibody.
F and G) KC3AC1 cells were stimulated with 10 nM IGF-1 for 0 to 30 min alone or in the presence of 10 µM U_{0126} or 10 µM Ly294002 (Ly) for 5 min. 30 µg protein lysates were submitted to direct WB using anti-phospho-p44/42 (F) or anti-phospho-AKT antibodies (G). Protein loadings were normalized with the corresponding antibodies.

Figure 6: GH and IGF-1 stimulate ionic transport in KC3AC1 cells
KC3AC1 cells seeded on collagen I-coated Transwell filters were starved for 24 h in minimum medium and treated or not (Basal) for 24 h with 100 ng/ml GH alone or with 10 µg/ml Peg (A-C). Similar experiments after 24 h starvation in minimum medium with insulin omission were performed with 10 nM IGF-1 treatments (D-F). Supernatants were recovered from the apical and basolateral compartments and Na^+, Cl^- and K^+ concentrations were measured. Ionic gradients representing the differences between basolateral versus apical Na^+ and Cl^- concentrations or the differences between apical versus basolateral K^+ concentrations were calculated. Results are mean ± SEM of independent determinations and represent fold induction above basal ionic gradient. (A = apical; B = basolateral * $p<0.05$, ** $p<0.01$, *** $p<0.001$).
A-C) Basal Na^+, Cl^- and K^+ concentration gradients in mmol/L/24 h were 4.40 ± 0.61, 3.60 ± 0.34 and 1.22 ± 0.21, respectively; n = 10.
D-F) Basal Na^+, Cl^- and K^+ concentration gradients in mmol/L/24 h were 4.76 ± 0.43, 3.53 ± 0.33 and 1.46 ± 0.17, respectively; n = 13.

Figure 7: GH and IGF-1 increase the expression of specific target genes in KC3AC1 cells.
A) Induction of SOCS2, CIS and αENaC mRNA expression in KC3AC1 cells by GH. Cells were incubated in minimal medium 3 h before exposure to GH (100 ng/ml) for 24 h. mRNA expression was measured by quantitative real time PCR. Results expressed as amol/fmol of 18S are mean ± SEM of 6 independent determinations (* $P<0.05$, ** $P<0.01$, *** $P<0.001$).
B) Specific binding to a STAT5 response element located in the αENAC promoter region. The sequence of the STAT5-RE oligonucleotide is underlined in bold. Nuclear extracts (5 µg proteins) from GH-treated (lane 1) and untreated KC3AC1 cells (lane 3) were analyzed for binding to a double-stranded STAT5-RE oligonucleotide. After a 15-min incubation of proteins with 10^5 cpm of [^{32}P]-radiolabeled STAT5-RE, protein-DNA complexes were separated on a nondenaturing 4.5% polyacrylamide gel and detected by autoradiography. Specific complexes were identified by competition experiments in which 100 ng unlabeled STAT5-RE was added (lanes 2 and 4).
C) KC3AC1 cells were starved for 24 h in minimum medium without insulin and exposed to 10 nM IGF-1 for various periods of time. Relative expression levels of Sgk1 and αENAC transcripts were determined by quantitative real time PCR analysis. Results are mean ± SEM of 6 independent determinations and represent fold induction above basal arbitrary set at 1 (* $P<0.05$, ** $P<0.01$). Basal expression of Sgk1 is 0.386 ± 0.014 amol/fmol 18S, and of αENaC 0.143 ± 0.004 amol/fmol of 18S.

Figure 8: Proposed model of cooperative GH and IGF-1 action in cortical collecting duct cells.

Name	Accession number	Amplicon	Sense primer	Antisense primer
18S	X00686	66 bp	CCCTGCCCTTTGTACACACC	CGATCCGAGGGCCTCACTA
GHR	NM_010284	150 bp	CCAAGTGTCGTTCCCCTGA	TGGGTCCATTCATGAGCAATT
IGF-1	NM_010512	150 bp	CACCACAGCTGGACCAGAGAC	ACACTCATCCACAATGCCTGTC
IGF-1R	NM_010513	150 bp	CGGTGACTTCTGCTCAAATGC	GAATGGCGGATCTTCACGTAG
αENaC	NM_011324	150 bp	GGACTGGAAAATCGGCTTCC	TAGAGCAGGCGAGGTGTCG
Sgk1	AF205855	150 bp	TCACTTCTCATTCCAGACCGC	ATAGCCCAAGGCACTGGCTA
SOCS2	NM_007706	119 bp	GAGACTTTGCCACACCATTCTG	TCACAGGGTACCCCAAAACG
CIS	AK_170877	150 bp	CTCCTACCTTCGGGAATCTGG	ACGGGTGGTTTTGACTGACAG
MR	M36074	153 bp	ATGGAAACCACACGGTGACCT	AGCCTCATCTCCACACACCAAG

Supplemental Table 1: Primer sequences of genes analyzed in RT-PCR and quantitative real-time PCR

The abbreviations of the murine genes, their full name, their GENBANK or NCBI accession number and 5' to 3' nucleotide sequences of the sense and antisense primers are presented.

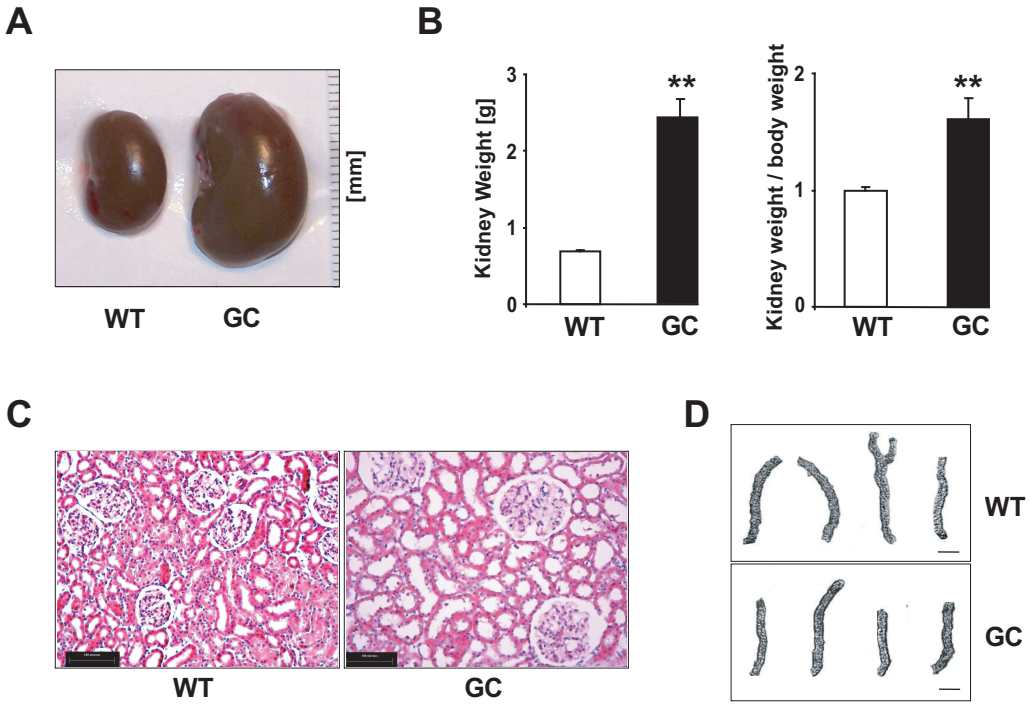

Figure 1

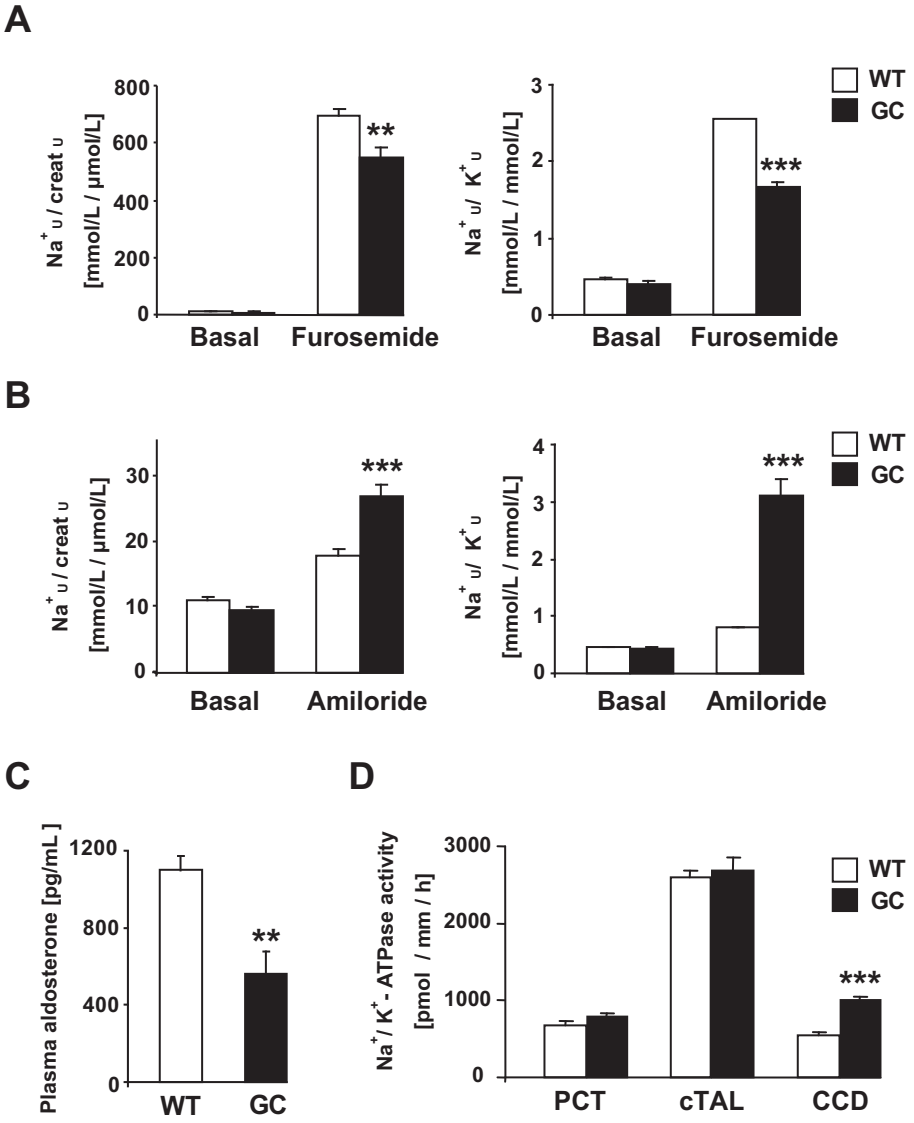

Figure 2

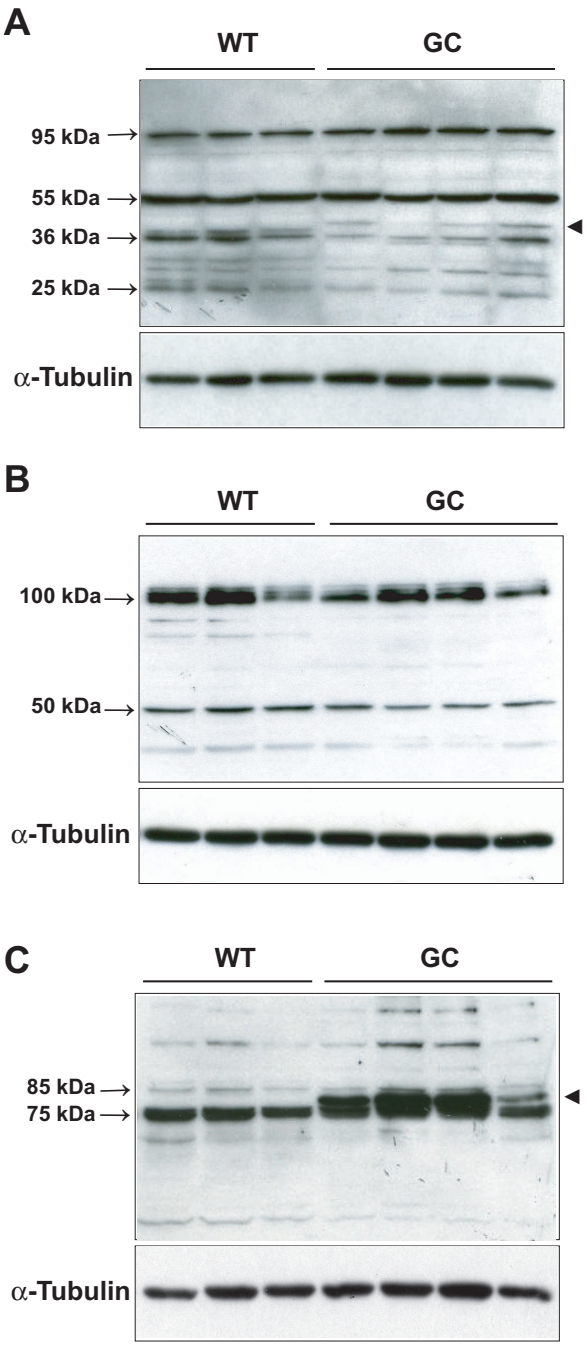

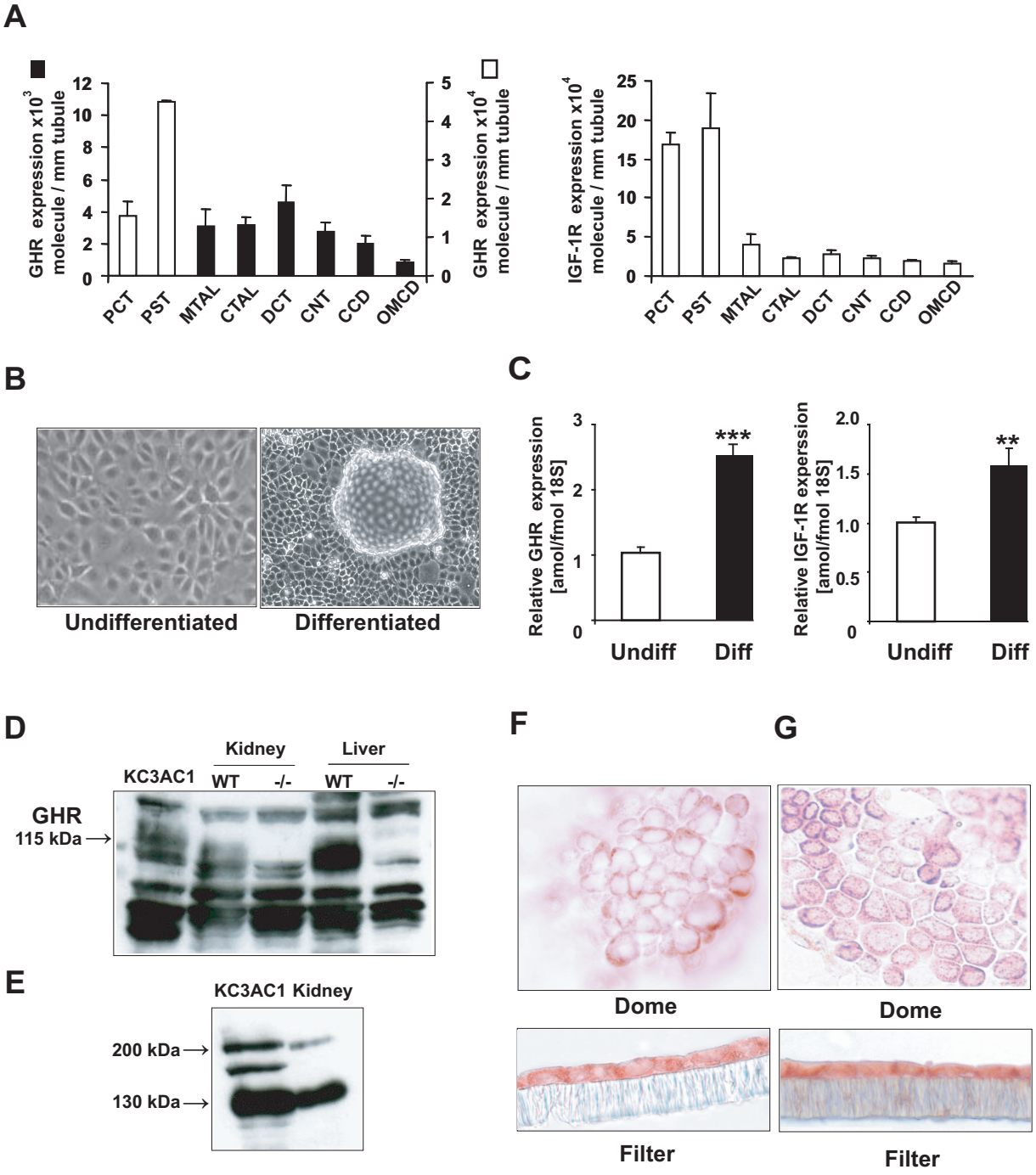

Figure 4

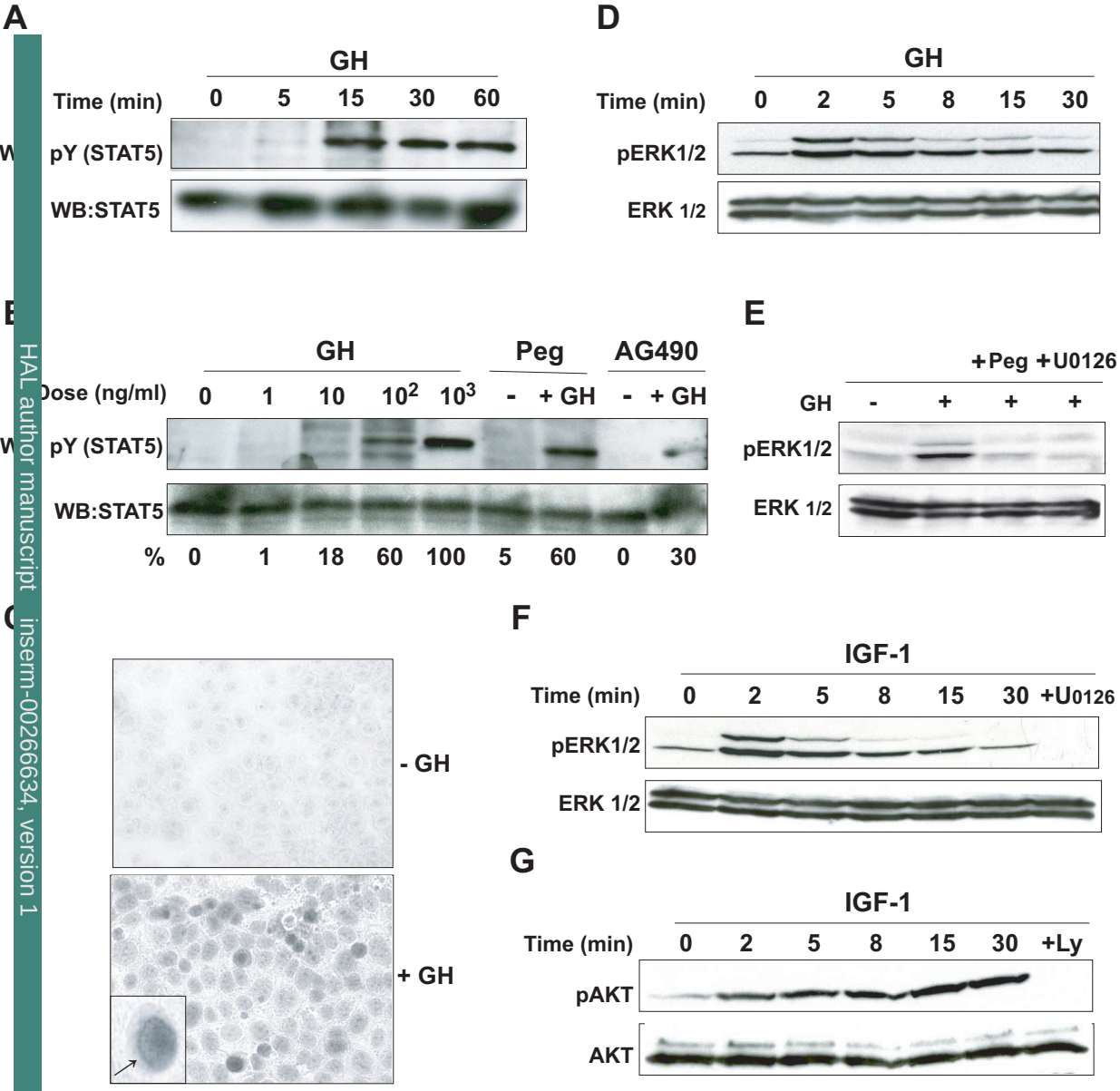

Figure 5

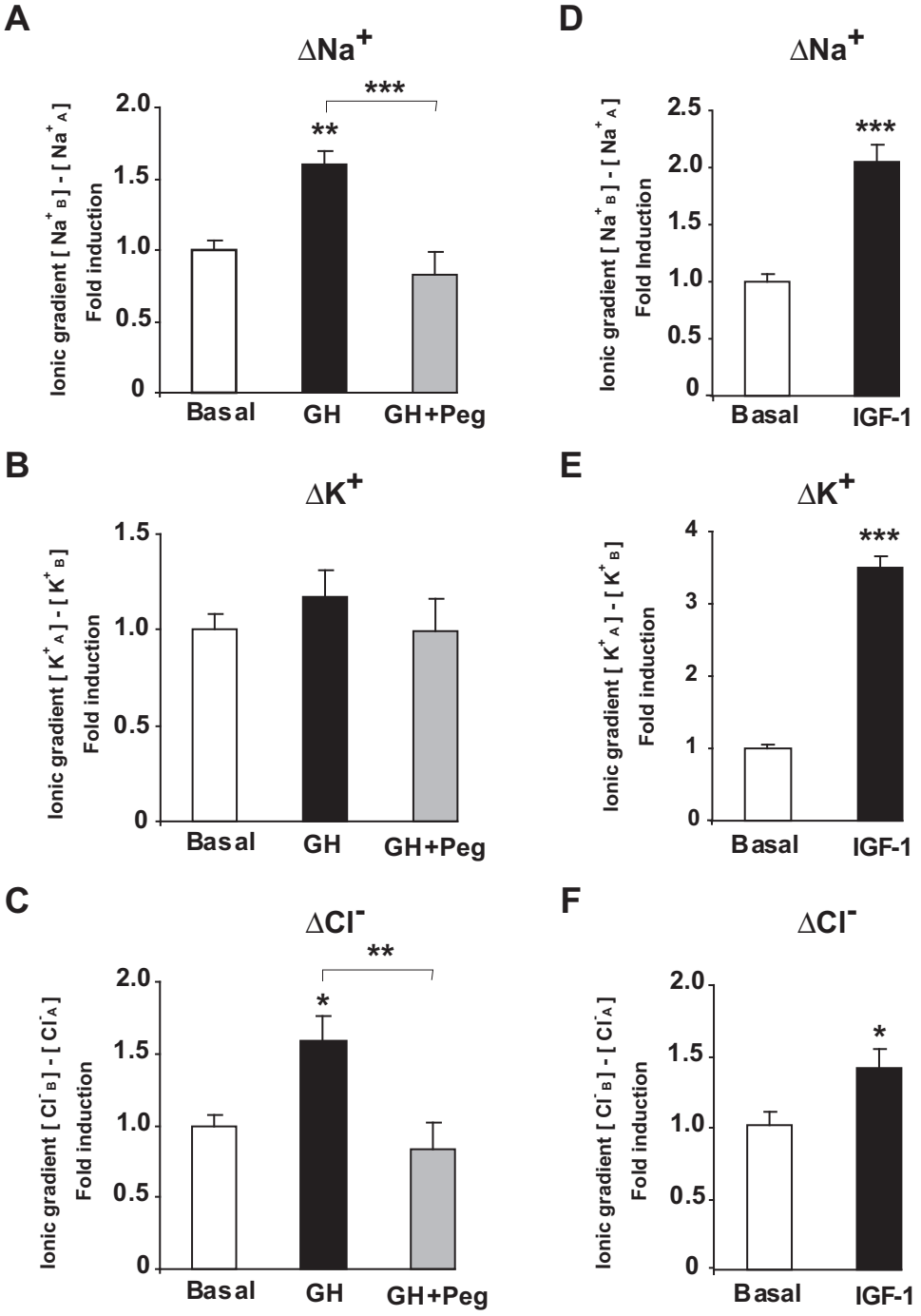

Figure 6

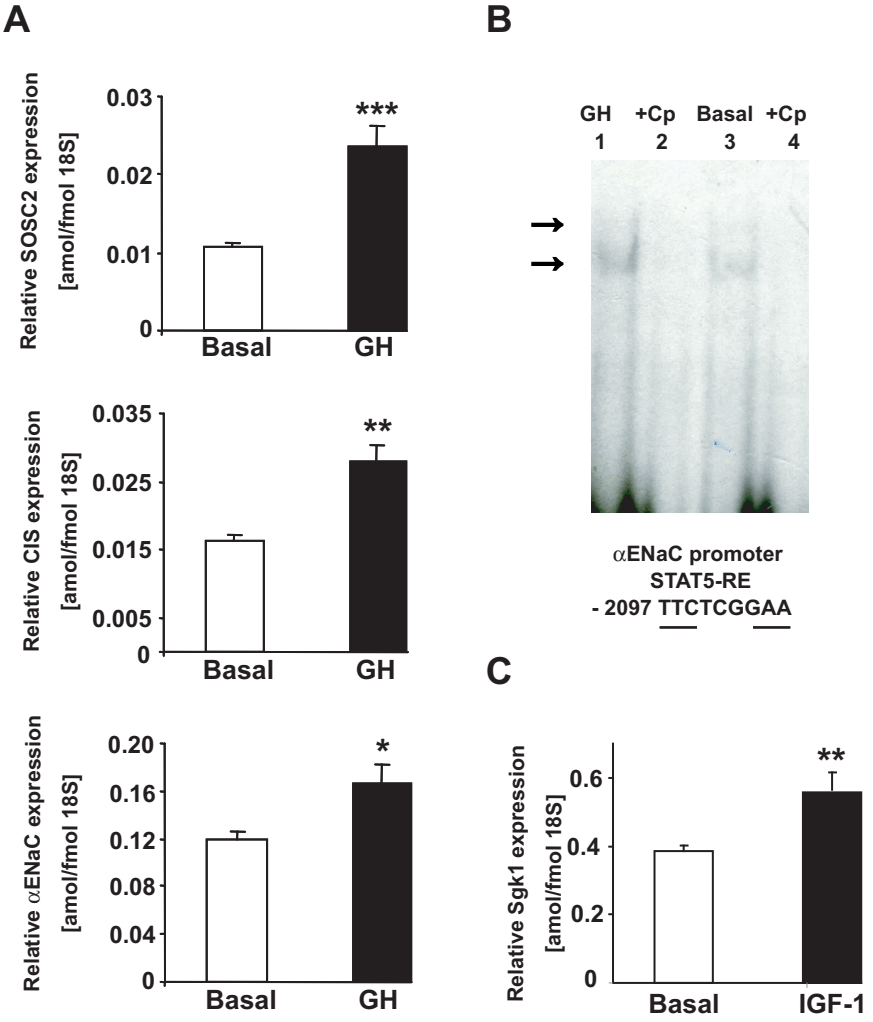

Figure 7

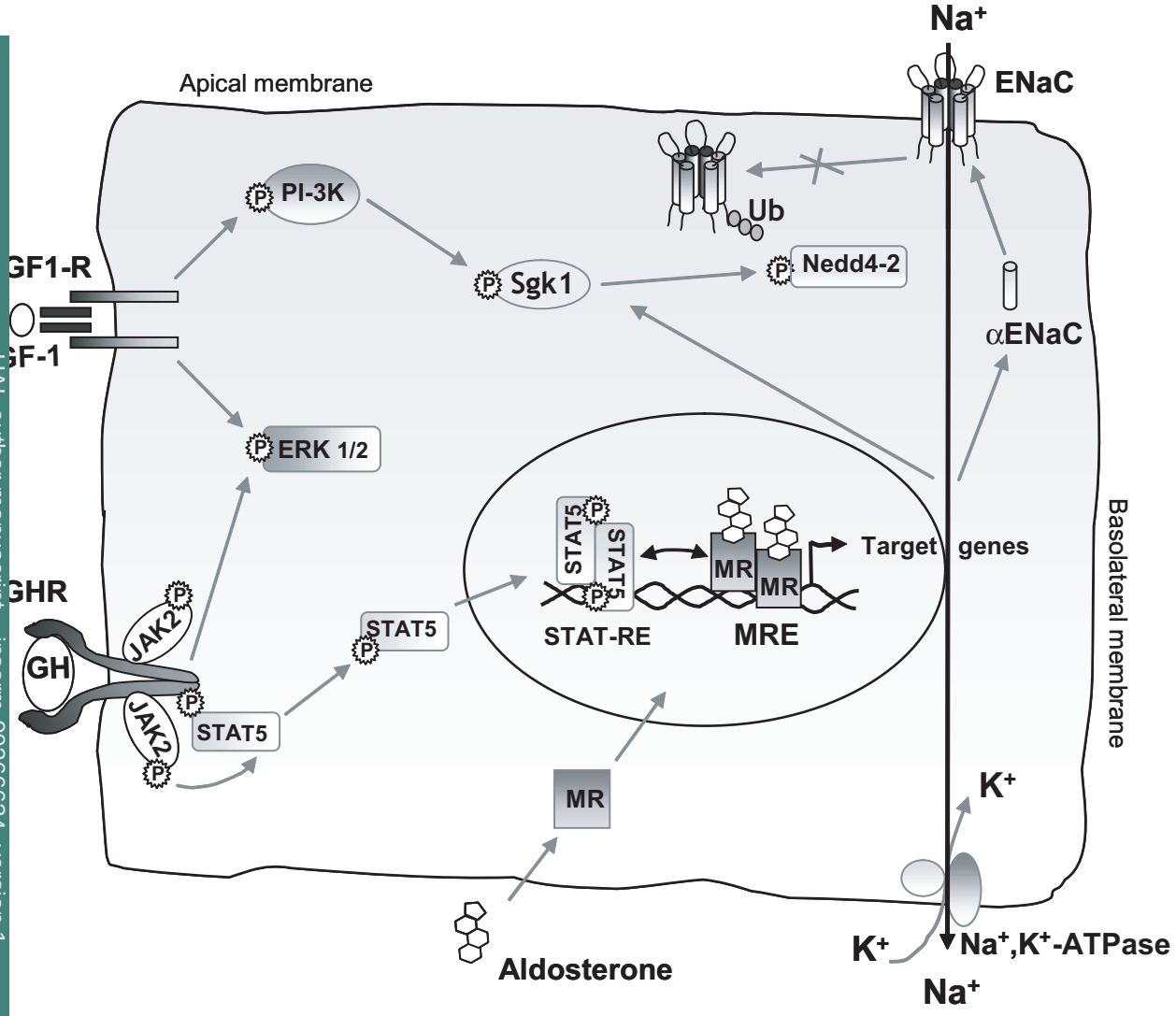

Figure 8